J. Phys. Chem. B **2003,** *107,* 659−663

Field-Effect Transistors Based on Single Semiconducting Oxide Nanobelts

Michael S. Arnold,[†] Phaedon Avouris,*[,†] Zheng Wei Pan,[‡] and Zhong L. Wang[‡]

IBM Research Division, T. J. Watson Research Center, Yorktown Heights, New York 10598 and School of Materials Science and Engineering, Georgia Institute of Technology, Atlanta, Georgia 30332-0245

Received: September 30, 2002

We have fabricated field-effect transistors (FETs) based on single SnO_2 and ZnO nanobelts of thicknesses between 10 and 30 nm. Switching ratios as large as 6 orders of magnitude and conductivities as high as 15 $(\Omega\ cm)^{-1}$ are observed. Annealing SnO_2 nanobelt FETs in an oxygen-deficient atmosphere produces a negative shift in gate threshold voltage, indicating doping by the generation of surface oxygen vacancies. This treatment provides an effective way of tuning the electrical performance of the nanobelt devices. The ability of SnO_2 FETs to act as gas sensors is also demonstrated. SnO_2 FETs with lengths of about 500 nm or less show an anomalous behavior where the conductance cannot be modulated by the gate. ZnO nanobelt FETs are sensitive to ultraviolet light. Both photogeneration of electron−hole pairs and doping by UV induced surface desorption contribute to the conductivity.

1. Introduction

Semiconducting transition and rare-earth metal oxides are attracting significant attention as candidates for chemical and environmental sensors.[1−4] This is because their electrical conductivity depends sensitively on the nature and concentration of adsorbed species on their surfaces. The key characteristics of these oxides are (a) cations with mixed valence and (b) oxygen vacancies. The latter are responsible for the observed high sensitivity of the electrical properties to the presence of adsorbed molecules and allow the tuning of the conductance of the oxide. Recently, nanobelt structures of a group of semiconducting oxides have been synthesized,[5,6] which are structurally perfect and geometrically uniform. The nanobelts have widths of 30−300 nm, thicknesses of 10−30 nm, and lengths of up to a few millimeters.

By forming metal electrode/nanostructure electrical contacts and capacitively coupling the nanostructure to a near by gate electrode, a field-effect transistor (FET) is produced that allows the exploration of new aspects of the physical and chemical properties of the nanostructures.[7−9] In this work, we demonstrate the fabrication of nanoscale FETs using SnO_2 and ZnO nanobelts as the FET channels, analyze their I−V characteristics, and demonstrate the sensitivity of the SnO_2 nanobelt conductance to gas exposure.

2. Experimental Procedure

Single-crystalline SnO_2 and ZnO nanobelts of thicknesses between 10 and 30 nm were synthesized by thermal evaporation of oxide powders in an alumina tube without the presence of a catalyst.[5] Large bundles of either SnO_2 or ZnO nanobelts were dispersed in ethanol by ultrasonication until mostly individual nanobelts were isolated. These ethanol dispersions were dried onto a SiO_2/Si substrate for imaging by noncontact mode AFM. SnO_2 field-effect transistors were fabricated by depositing SnO_2 nanobelt dispersions onto SiO_2 / Si (p^+) substrates, followed by treatment in an oxygen atmosphere at 800 °C for 2 h. The SiO_2/Si substrates were then spin-coated with PMMA, baked, exposed to electron-beam lithography for the definition of electrode arrays, and developed. A 30-nm-thick layer of titanium was deposited by electron-beam evaporation to serve as the source and drain electrodes, and the remaining PMMA was lifted off in hot acetone.

An alternative way of contacting the nanostructures was applied to ZnO nanobelts. In this case, field-effect transistors were fabricated by depositing dispersed ZnO nanobelts on predefined gold electrode arrays. In both cases, the SiO_2 gate dielectric thickness was 120 nm, and the back gate electrode was fabricated by evaporation of gold on the Si (p^+) side of the substrate. Also, in both fabrication schemes, the electrode arrays were variably spaced. They included electrode gaps as small as 100 nm and as large as 6 μm.

3. Results and Discussion

3.1. Field Effect Transistors. Both SnO_2 and ZnO nanobelts formed field effect transistors. A typical SnO_2 field effect transistor pretreated in a 1atm oxygen atmosphere at 800 °C (Figure 1a) demonstrated a gate-threshold voltage of −2.5 V, a current switching ratio I(ON)/I(OFF) of nearly 10 000, and (ignoring voltage drops at the Ti contacts) a peak conductivity of 8.14 $(\Omega\ cm)^{-1}$. Measured conductivities ranged from 4 to 15 $(\Omega\ cm)^{-1}$. The typical leakage conductance between our electrodes under ambient conditions measured between 20 and 80 pS and was gate-bias independent. In most cases, the switching ratios of our FETs were limited by this background conductivity. From an analysis of the transconductance, dI_d/dV_g, for gate biases above the threshold bias, the electron mobility of an n-type field effect transistor can be estimated if the geometry of the device is known.[11] Without subtracting voltage drops at the contacts, from analysis of Figure 1a the electron mobility in the SnO_2 nanobelt was estimated to be ~35 cm^2/V s. Other measured SnO_2 nanobelt FETs exhibited electron mobility ranging from 10 to 125 cm^2/V s. From four-probe measurements on other devices, the contact resistance between

* To whom correspondence should be addressed. E-mail: avouris@us.ibm.com.
[†] IBM Research Division.
[‡] Georgia Institute of Technology.

10.1021/jp0271054 CCC: $25.00 © 2003 American Chemical Society
Published on Web 12/28/2002

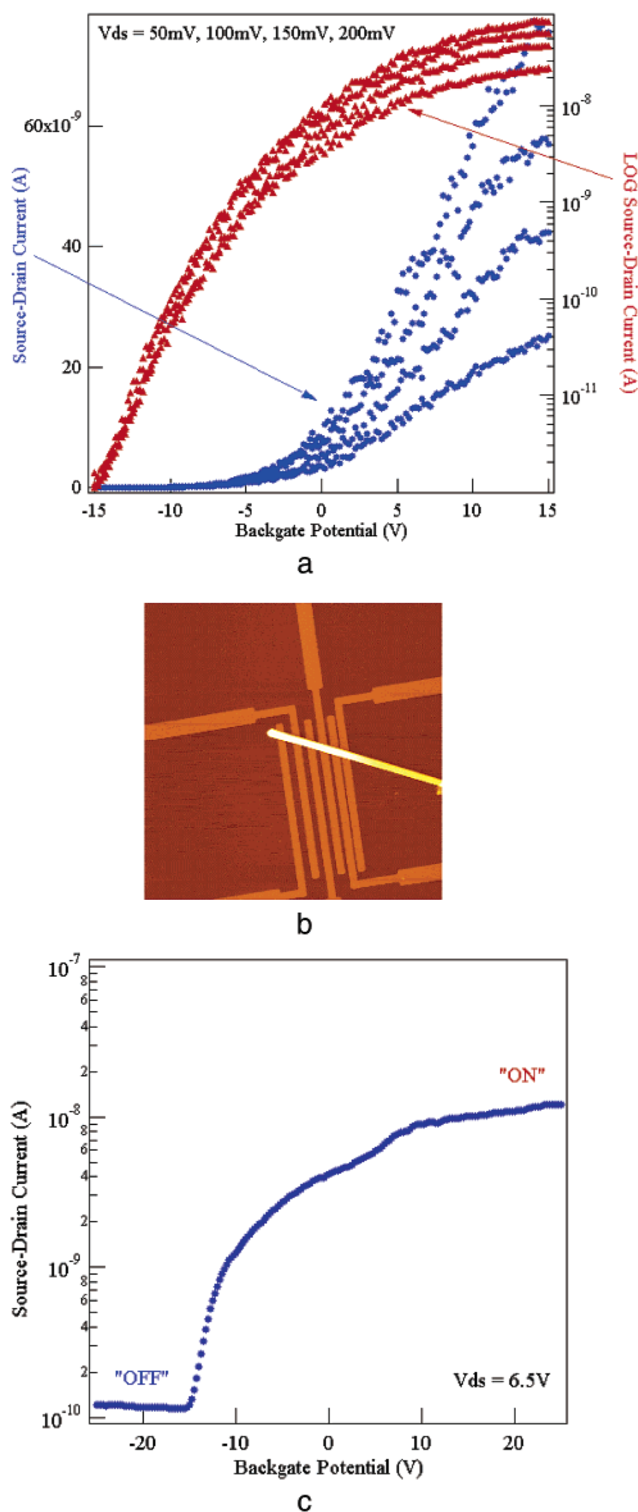

Figure 1. Nanobelt FET. (A) Source-drain current versus gate bias for a SnO_2 FET in ambient. (B) $(10\ \mathrm{um})^2$ NC-AFM image of ZnO FET across gold electrodes. (C) Source-drain current versus gate bias for a ZnO FET in ambient.

the Ti electrodes and the SnO_2 nanobelt was found to be on the same order of magnitude as the four-probe "ON" channel resistance. Thus, our calculations underestimate both conductivity and mobility by assuming the entire source drain potential is dropped across the nanobelt.

The alternative way of contacting the nanobelts by simply depositing them on top of prefabricated gold electrodes led to very resistive contacts. A typical ZnO field effect transistor (Figure 1b) showed a gate threshold voltage of −15 V, a switching ratio of nearly 100, and a peak conductivity of $1.25 \times 10^{-3}\ (\Omega\ \mathrm{cm})^{-1}$ (Figure 1c). A completely analogous behavior has been observed in the case of carbon nanotubes deposited on top of Au electrodes or covered by Ti electrodes.[10]

3.2. Sensitivity of the Electrical Properties of Nanobelts to Environment. Before electrical measurement, SnO_2 nanobelts are annealed in a 1 atm oxygen environment at 800 °C for 2 h. Without this treatment, the as-produced nanobelts exhibit no measurable conductivity for source-drain biases from −10 to +10 V and for gate biases from −20 to +20 V, whereas after this treatment the SnO_2 nanobelts exhibit considerable conductivity. The SnO_2 devices, with their conductivity activated, demonstrate electrical properties as described in section 3.1. By further annealing of the devices at lower temperatures in a vacuum, oxygen, or *ambient*, the electrical properties of the nanobelts can be tuned.

After annealing of the SnO_2 devices in a vacuum at 200 °C, the nanobelt conductivity is observed to increase along with an associated negative-shift in gate-threshold voltage. Smaller, additional increases in conductivity are observed after additional vacuum anneals. Eventually, the nanobelt behaves like a metal with the gate field being unable to affect the current flowing through the device. In contrast, annealing nanobelt devices in *ambient* at 200 °C leads to a decrease of the conductivity, along with a shift in the gate-threshold voltage in the opposite, positive direction (Figure 2a). The source-drain conductivity at zero gate bias spans 3 orders of magnitude from $0.09\ (\Omega\ \mathrm{cm})^{-1}$ after annealing at 200 °C in *ambient* to $75.3\ (\Omega\ \mathrm{cm})^{-1}$ after annealing at 250 °C in a vacuum. The changes in conductivity with low temperature annealing most likely result from variations in the number of oxygen species adsorbed on the SnO_2 surfaces or in the number of oxygen vacancies in the SnO_2 bulk with the amount of oxygen in the environment.[16−20] The number of equilibrium surface and bulk oxygen defects will be a function of the environmental oxygen partial pressure and temperature.[18−21] Annealing in a vacuum should decrease the number of adsorbed oxygen species and increase the number bulk oxygen vacancies, whereas annealing in oxygen or *ambient* should do the opposite. It is well established that bulk and surface oxygen vacancies in SnO_2 act as electron donors, which should increase SnO_2 conductivity and decrease the gate threshold voltage.[18−20] This is precisely what we observe.

It should be noted that the SnO_2 nanobelt conductivity is observed to increase and the gate threshold voltage is observed to decrease simply by taking a nanobelt device from ambient into vacuum without annealing (Figure 2a). Because the diffusion of bulk oxygen vacancies at room temperature will be limited,[17,20] this indicates that surface oxygen desorption is most likely taking place at this temperature. Because of their small dimensions, semiconducting oxide nanobelts will have on the order of 10^{20} surface oxygen sites per cubic centimeter of material.[19] Thus, even for partial changes in the concentration of adsorbed oxygen species, large changes in nanobelt conductivity can be observed.

As noted, annealing at 200 and 250 °C induces further changes in conductivity (Figure 2a). To account for this, either the surface or bulk nanobelt composition must change as a result of these annealing steps. Mizusaki[19] has argued that for temperatures below 900 °C the equilibrium bulk nonstoichiometry of SnO_2 will be insignificant in comparison to surface nonstoichiometry in samples of similar surface/volume ratios. This suggests that surface oxygen vacancies should control conductivity after 200 and 250 °C anneals. Annealing might

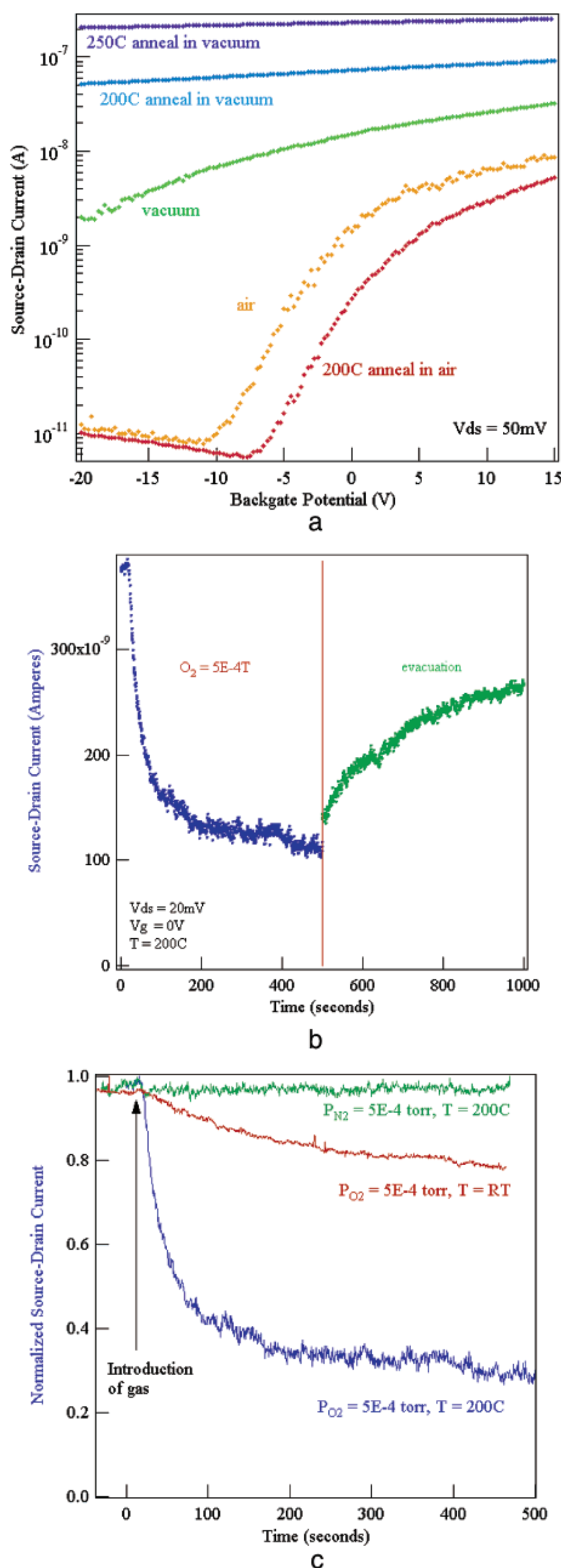

Figure 2. SnO_2 Nanobelt FET oxygen sensitivity. (A) Source-drain current versus gate bias for a SnO_2 FET after various treatments measured in this order: air, vacuum, 200 C vacuum anneal, 250 C vacuum anneal, 200 C air anneal. All measurements taken at room temperature with vacuum anneal measurements taken in a vacuum and air anneal measurements in air. (B) Source-drain current at zero gate bias of a hot 200C SnO_2 FET as a function of time with exposure to air and subsequent recovery. (C) Comparison of source-drain current at zero gate bias of a SnO_2 FET in nitrogen and oxygen.

also desorb species other than oxygen from the nanobelt surfaces. Water could act as a mask on the nanobelt surface, decreasing sensitivity to environmental oxygen until removed.

The sensitivity of the FET to gas exposure can also be demonstrated by measuring the SnO_2 nanobelt conductivity as a function of time after introduction of oxygen. The conductivity of a hot 200 °C SnO_2 nanobelt in a vacuum is observed to decay to about $^1/_3$ its initial value after exposure to oxygen at a pressure of 5×10^{-4} Torr (Figure 2b). The exponential time constant for this decay is 37.2 s. After removal of the oxygen, the conductivity recovers about twice as slow, with a time constant of 76.5 s. In contrast, the conductivity of the same SnO_2 nanobelt at the same temperature is invariant upon exposure to nitrogen at the same pressure (Figure 2c). Exposure of the nanobelt to 5×10^{-4} Torr oxygen at room temperature leads to the decay of the conductivity at a much slower rate with a time constant of 156.9 s, reflecting the activated nature of the oxygen desorption processes.[19] At room temperature, a smaller percentage of surface vacancy sites are likely to be affected; thus, a smaller current change is produced.[19]

3.3. Channel Length Dependence of the Transistor Operation. As we indicated in the Experimental Section, variable spacing electrodes were fabricated to contact the nanobelts. Thus, SnO_2 nanobelts were contacted with electrodes spaced at 127, 254, 1080, and 1840 nm, and the dependence of the conductance of the nanobelts on gate bias was studied as a function of electrode spacing. A nonlinear relationship between the conductance and electrode spacing was found. The conductance of the SnO_2 nanobelt was modulated less effectively between short electrode gaps than between large electrode gaps. Between electrodes spaced 1080 and 1840 nm apart, sweeping the gate voltage from −15 to +15 V (source-drain bias 0.05 V) modulated the conductance by more than 5 orders of magnitude from less than 10^{-11} S to greater than 10^{-6} S (Figure 3a). Between electrodes spaced 127 and 254 nm apart, sweeping the gate over the same range of voltages only modulated the conductance of the same nanobelt by less than 1 order of magnitude. Considering the SnO_2 nanobelt as a resistor, one would expect the conductance to scale inversely with length, regardless of gate bias. By normalizing the conductance by electrode spacing, the nonlinear effects can be best observed (Figure 3b). At large positive gate biases near +15 V, the conductivity of the nanobelt is roughly the same for each segment. The small variations observed of less than 1 order of magnitude in conductivity are most likely due to variations in the contact resistances to each segment. The length dependence becomes evident at negative gate biases near −15 V, where the conductivity of the nanobelt varies by more than 5 orders of magnitude depending on electrode spacing. What is observed is that the current in short segments cannot be turned "OFF" by the gate, whereas in long segments, the current can be modulated by the gate field. It should be noted that the effects observed here are not the typical "short channel effects" well-known in metal-oxide-semiconductor field effect transistors (MOSFETs).[11] Other SnO_2 nanobelts contacted with variably spaced electrodes exhibit the same short channel effects. It is consistently observed that the conductivity of devices between electrodes spaced far apart is effectively modulated by a gate bias (by as much as 6 orders of magnitude), whereas the conductivity of devices between closely spaced electrodes is not effectively modulated. Qualitatively, the transition between these two regimes is broad and centered near 500 nm.

3.4. Photoconductivity of Nanobelts. Ultraviolet light irradiation of ZnO in air is observed to result in a significant

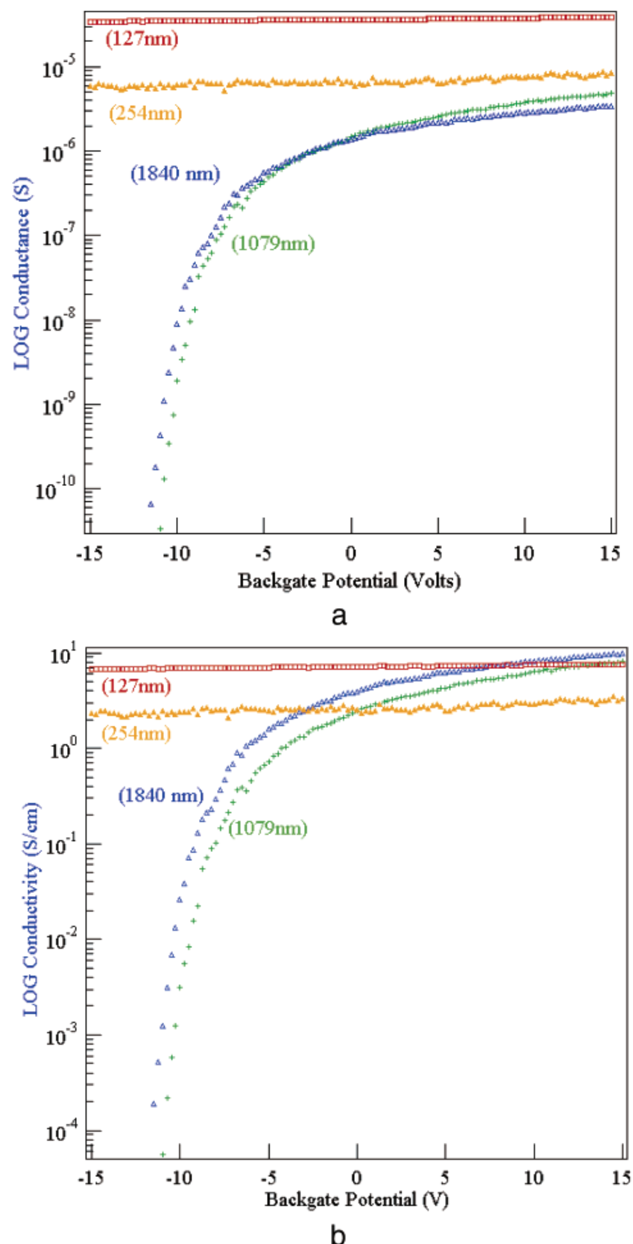

Figure 3. SnO_2 Nanobelt FET $I-V_g$ curves as a function of back gate bias and electrode spacing. (A) Source-drain conductance versus back gate voltage for electrode spacing of 127, 254, 1079, and 1840 nm. (B) Conductance normalized by area and electrode length versus back gate voltage for the same electrode spacings. Short channel effects are manifested at negative gate biases in which the back gate no longer modulates channel conductivity.

increase of the conductivity. Light with a wavelength of 350 nm ($E_\lambda = 3.54$ eV) was used, exceeding the direct band-gap of ZnO, which is of 3.2 eV.[13,15] The increase in the conductivity results from both photogeneration of electron−hole pairs as well as doping by UV light-induced surface desorption.[12−15] These processes could be observed by introducing a shutter between the light source and the ZnO nanobelt so that the flux of UV photons could be turned "ON" and "OFF". In the insert to Figure 4, the conductivity can be observed to rise and fall in response to opening and then closing the shutter. After the establishment of a steady state with the UV light "ON", the decay of conductivity after closing the shutter reveals two regimes (Figure 4). The first regime is characterized by a sharp drop in conductivity immediately after the shutter is closed. This sharp drop is due to the recombination of photogenerated electron−hole pairs. The second regime is characterized by the slow decay of current. This slow gradual change suggests a surface chemical reaction.

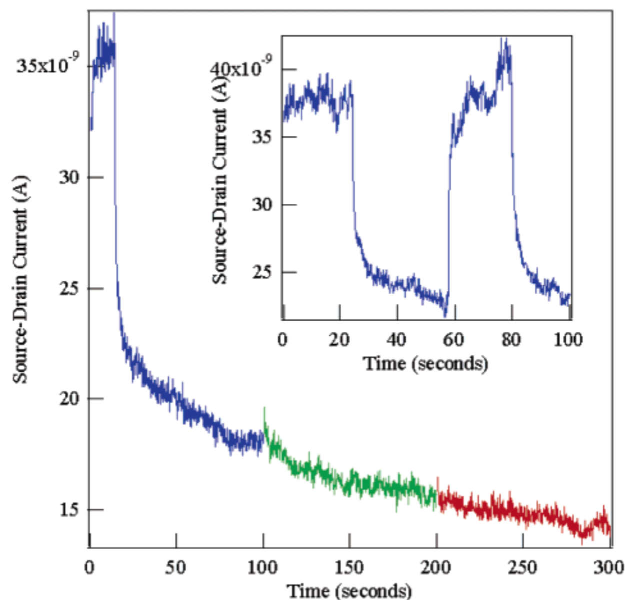

Figure 4. ZnO nanobelt response to UV light. Source-drain current versus time at zero-gate bias and a source drain potential of 6.5 V. The initial state of the nanowire in these responses was one of steady state with a 350 nm light source ON. Insert: Source-drain current versus time as a 350 nm source is cycled OFF and ON. Figure: Source-drain current versus time plot depicting two regimes of current decay after UV stimulation is turned OFF. The first regime is the sharp drop in current which most likely represents the cessation of photo generation of carriers. The second regime is the slow decay of current. This may be due to recovery of surface chemistry modified by UV exposure.

Similar effects have been observed in ZnO thin films.[12−15] In one thin film model, during UV exposure, photogenerated holes react with negatively charged adsorbed oxygen species liberating O_2,[12,13] while in another model, photogenerated holes react with negatively charged carbon dioxide species liberating CO_2.[14,15] In both models after the UV light has been turned "OFF", the surface conductivity slowly decays as oxygen is re-adsorbed increasing the number of electron acceptors in the n-type material.

4. Conclusion

FETs made from single crystalline SnO_2 and ZnO nanobelts have been fabricated. They have switching ratios as large as 6 orders of magnitude, conductivity as high as 15 $(\Omega\ \mathrm{cm})^{-1}$, and electron mobility as large 125 cm^2/V s. Furthermore, SnO_2 nanobelts can be doped with surface oxygen vacancies by annealing them in reduced oxygen environments. This process increases the conductivity and drastically decreases the gate threshold voltage, indicating the feasibility of tuning device characteristics by controlling adsorbed oxygen species. Short channel effects have been observed in SnO_2 nanobelts showing the inability of the gate electrode to modulate source-drain channel conductivity in nanobelts shorter than about 500 nm. In ZnO nanobelts, which have a direct band gap, two processes are observed to contribute to photoconductivity. The first process involves the photogeneration of electron−hole pairs, whereas the second process most likely involves chemical desorption from the ZnO surface by exposure to UV light.

Acknowledgment. M.S.A. thanks IBM for a summer internship**.** We also thank J. Appenzeller and R. Martel for valuable discussions and B. Ek for expert technical assistance.

References and Notes

(1) Morrison, S. R. *Sens. Actuators* **1982**, *2*, 329.
(2) Sharma, R. K.; Chan, P. C. H.; Tang, Z.; Yan, G.; Hsing, I.-M.; Sin, J. K. O. *Sens. Actuators, B* **2001**, *72*, 160.
(3) Hahn, S. H.; Barsan, N.; Weimar, U. *Sens. Actuators, B* **2001**, *78*, 64.
(4) Lin, H.-M.; Tzeng, S.-J.; Hsiau, P.-J.; Tsai, W.-L. *NanoStr. Mater.* **1998**, *10*, 465.
(5) Pan, Z. W.; Dai, Z. R.; Wang, Z. L. *Science* **2001**, *291*, 1947.
(6) Wang, Z. L.; Kang, Z. C. *Functional and smart materials—structural evolution and structure analysis*; Plenum Press: New York, 1998.
(7) Cui, Y.; Lieber, C. M. *Science* **2001**, *291*, 851.
(8) Collins, P. C.; Arnold, M. S.; Avouris, Ph. *Science* **2001**, *292*, 706.
(9) Kong, J.; Franklin, N.; Wu, C.; Pan, S.; Cho, K. J.; Dai, H. *Science* **2000**, *287*, 622.
(10) Avouris, Ph. *Chem. Phys.* **2002**, *281*, 429.
(11) Streetman, B. G. *Solid State Electronic Devices*, 4th ed.; Prentice Hall: New York, 1995.
(12) Zhang, D. H. Mater. *Chem. Phys.* **1996**, *45*, 248.
(13) Bonasewicz, P.; Hirschwald, W.; Neumann, G. *J. Electrochem. Soc.* **1986**, *133*, 2270.
(14) Shapira, Y.; Cox, S. M.; Lichtman, D. *Surf. Sci.* **1976**, *54*, 43.
(15) Tansley, T. L.; Neely, D. F. *Thin Solid Films* **1984**, *121*, 95.
(16) Advani, G. N.; Kluge-Weiss, P.; Longini, R. L.; Jordan, A. G. *Int. J. Electron.* **1980**, *48*, 403.
(17) Kamp, B.; Merkle, R.; Maier, J. *Sens. Actuators, B* **2001**, *77*, 534.
(18) Samson, S.; Fonstad, C. G. *J. Appl. Phys.* **1973**, *44*, 4618.
(19) Mizusaki, J.; Koinuma, H.; Shimoyama, J.-I.; Kawasaki, M.; Fueki, K *J. Solid State Chem.* **1990**, *88*, 443.
(20) Göpel, W.; Schierbaum, K.; Wiemhöfer, H.-D. *Solid State Ionics* **1989**, *32*, 440.
(21) Flynn, C. P. *Point Defects and Diffusion*; Clarendon Press: Oxford Press, 1972.